PHOTONICS Research

Compact, submilliwatt, 2 × 2 silicon thermo-optic switch based on photonic crystal nanobeam cavities

HUANYING ZHOU,[1] CIYUAN QIU,[1,3] XINHONG JIANG,[1] QINGMING ZHU,[1] YU HE,[1] YONG ZHANG,[1] YIKAI SU,[1,4] AND RICHARD SOREF[2]

[1]State Key Lab of Advanced Optical Communication Systems and Networks, Department of Electronic Engineering, Shanghai Jiao Tong University, Shanghai 200240, China
[2]Engineering Department, University of Massachusetts, Boston, Massachusetts 02125, USA
[3]e-mail: qiuciyuan@sjtu.edu.cn
[4]e-mail: yikaisu@sjtu.edu.cn

Received 17 November 2016; revised 23 January 2017; accepted 26 January 2017; posted 27 January 2017 (Doc. ID 280900); published 28 February 2017

We propose and experimentally demonstrate a 2 × 2 thermo-optic (TO) crossbar switch implemented by dual photonic crystal nanobeam (PCN) cavities within a silicon-on-insulator (SOI) platform. By thermally tuning the refractive index of silicon, the resonance wavelength of the PCN cavities can be red-shifted. With the help of the ultrasmall mode volumes of the PCN cavities, only ~0.16 mW power is needed to change the switching state. With a spectral passband of 0.09 nm at the 1583.75 nm operation wavelength, the insertion loss (IL) and crosstalk (CT) performances were measured as IL(bar) = −0.2 dB, CT(bar) = −15 dB, IL(cross) = −1.5 dB, and CT(cross) = −15 dB. Furthermore, the thermal tuning efficiency of the fabricated device is as high as 1.23 nm/mW.

OCIS codes: (130.3120) Integrated optics devices; (230.5298) Photonic crystals; (130.4815) Optical switching devices.

https://doi.org/10.1364/PRJ.5.000108

1. INTRODUCTION

Optical switching is currently perceived as a promising technique in optical communication systems including optical add–drop multiplexing (OADM) systems and optical cross-connects (OXCs) [1,2]. The cost-effective and power-efficient optical switching networks require optical switches with low power consumption and high capacity [3,4]. A 2 × 2 optical crossbar switch, capable of routing an optical signal from an input port to an unoccupied output port, is a key component for these optical switching networks [5]. Such 2 × 2 units, when cascaded and interconnected, are the building blocks that enable a high-radix $N \times N$ switch fabric offering large numbers of routing channels [6–8].

Silicon-on-insulator (SOI) offers a very attractive platform to implement large-scale optical switches due to its high index contrast and compatibility with complementary metal oxide semiconductor (CMOS) foundry technology [9–12]. Furthermore, silicon has a large thermo-optic (TO) coefficient ($dn/dT = 1.86 \times 10^{-4}$ K^{-1} at 1.55 μm wavelength) [13]. To date, various schemes have been demonstrated to implement compact, low-loss, and low-power TO switches based on silicon microring resonators (MRRs), Mach–Zehnder interferometers (MZIs), and so on [14,15]. The main requirement for TO switches is a small device footprint and low switching power, which is affected by the optical mode volume and the light–matter interaction in the optical devices [16,17].

Compared with previous device configurations, a photonic crystal nanobeam (PCN) cavity may be an effective solution to achieve low-power optical switches, albeit resonant rather than broadband. In a PCN cavity, photons are strongly confined within a small area and light–matter interaction is highly enhanced [18–23]. Thus, PCN cavities have ultrasmall mode volumes, leading to a compact device footprint and low switching power in the TO switches based on PCN cavities. The feasibility of a 2 × 2 optical switch based on PCN cavities was analyzed by coupled mode theory and numerically demonstrated using finite-difference time-domain (FDTD) simulations [24]. Recently, we fabricated such a PCN-cavities-based 2 × 2 TO switch and presented preliminary experimental results, realizing a high Q-factor, a high extinction ratio at the through port, and a low insertion loss (IL) at the drop port, but not achieving the resonance-wavelength tuning [25].

In this paper, we perform a complete study of the proposed 2 × 2 TO switch based on dual silicon PCN cavities in terms of

device design, fabrication, and thermal tuning of the resonance wavelength. The experimental device performance is in good agreement with numerical simulations [24]. To our knowledge, this is the first nanobeam crossbar switch. By thermally tuning the refractive index of silicon, the resonance wavelength of the PCN cavities can be red-shifted by ~1.64 nm from 1583.75 to 1585.39 nm with an applied power varied from 0 to 1.31 mW. Only ~0.16 mW is required to switch from the cross state to the bar state and the thermal tuning efficiency of the TO switch is ~1.23 nm/mW, which is higher than that of recently reported typical silicon 2 × 2 TO switching devices with metal heaters. This is mainly due to the ultrasmall mode volumes of the PCN cavities. The observed IL and crosstalk (CT) of this TO switch reveal high performance as is detailed below.

2. DEVICE DESIGN AND FABRICATION

The proposed 2 × 2 silicon TO switch is a compact four-port system consisting of two cascaded PCN cavities as illustrated in Fig. 1(a). In each PCN cavity, the central nanobeam waveguide is side-coupled to two identical bus waveguides with equal coupling strengths to form a three-waveguide (3W) directional coupler. The central nanobeam waveguide etched with an array of air-holes forms a Fabry–Perot (F–P) cavity, which consists of a central-taper section and two side-reflector sections. The central-taper section with 13 holes is optimized to reduce the scattering loss and provide high phase matching between the photonic crystal fundamental Bloch mode and the waveguide mode. The side-reflector sections are designed as two symmetrical mirrors to reflect light to the central-taper section. To achieve a relatively high Q-factor and a large extinction ratio, the widths of the nanobeam waveguide and the identical bus waveguides are optimized to be 0.565 and 0.6 μm, respectively. The gap between the nanobeam waveguide and the bus waveguides is 0.21 μm.

The optical field distribution of a single PCN 3W structure is shown in Fig. 2(a) based on the Lumerical 2.5D variational FDTD simulation with a mesh size of 25 nm in the x direction and 25 nm in the y direction, with x, y, z directions indicated in Fig. 1(a). It can be seen that the light power concentrates in an ultrasmall area and the effective length for the thermal tuning is only ~2 μm as expected. Figure 2(b) shows the simulated

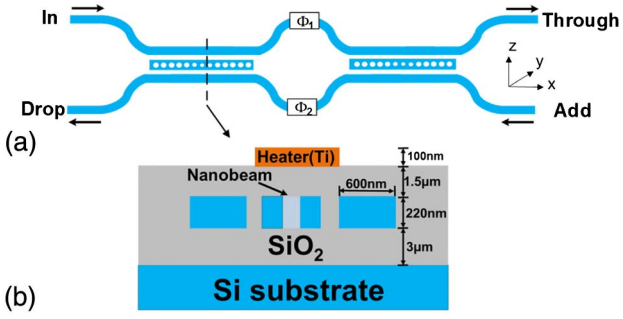

Fig. 1. (a) Schematic diagram of the proposed 2 × 2 TO switch based on dual PCN cavities. The phase difference between the two arms ($\Phi_1 - \Phi_2$) is equal to π. (b) Cross-section view of the coupled region in one half of the proposed 2 × 2 TO switch.

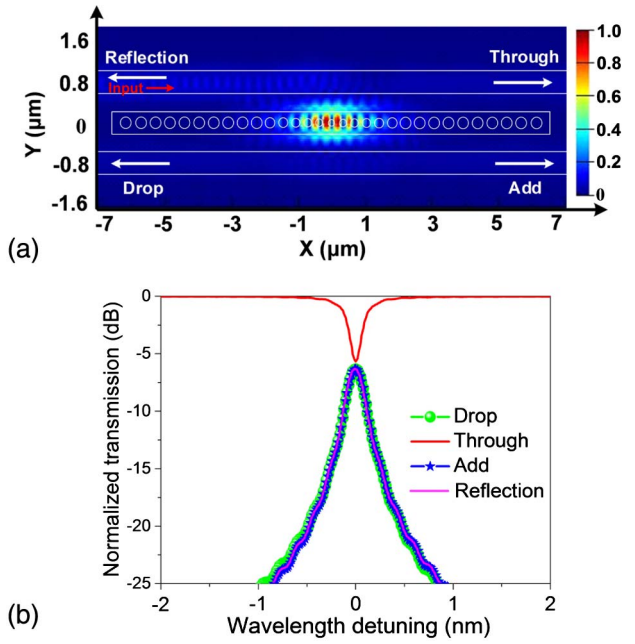

Fig. 2. (a) Calculated electric field distribution of a single PCN 3W structure at the resonant wavelength based on 2.5D variational FDTD simulation. (b) Simulated transmission spectra of a single PCN 3W structure.

transmission spectra of a single PCN 3W structure. The transmission efficiency at each port is about 25%; thus, an ~6 dB extinction ratio is achieved at the through port.

To realize a high drop-port transmission at the cross state of the TO switch, two identical PCN 3W structures are cascaded with a properly chosen phase difference between the two connecting bus waveguides. Based on the coupled mode theory, most light power goes to the drop port if the phase difference between the two arms $|\Phi_1 - \Phi_2|$ is equal to π radians [26,27], where the device works at the cross state. The switching state can be changed to bar state by tuning the resonant wavelengths of the PCN cavities with the help of the embedded microheaters as shown in Fig. 1(b). Since the mode volume of a resonant cavity is less than 1/10 of that in [27], the PCN 3W structure in this work enables ultra-low switching power in the TO switch.

The designed device was fabricated on an SOI wafer with a 220 nm thick top silicon layer and a 3 μm thick buried dioxide layer. The device was fabricated by e-beam lithography and reactive ion etching (RIE). A thick layer of 1.5 μm of silicon dioxide was deposited upon the exposed top surface of both 3W regions by plasma-enhanced chemical vapor deposition (PECVD). First, a 100 nm thick patterned titanium layer was sputtered on that oxide to form the microheaters. Then a 2 μm thick aluminum layer was sputtered to form the contact pads. The connecting arms between the 3W structures have a third microheater. The micrograph of the fabricated 2 × 2 TO switch based on dual PCN 3W structures is shown in Fig. 3(a). The overall optical device was fabricated with a footprint of 30 μm × 150 μm. The lengths of heater #1 and heater #2 for nanobeam resonance wavelength shifts are ~13 μm, and the length of heater #3 for a π phase difference is ~150 μm.

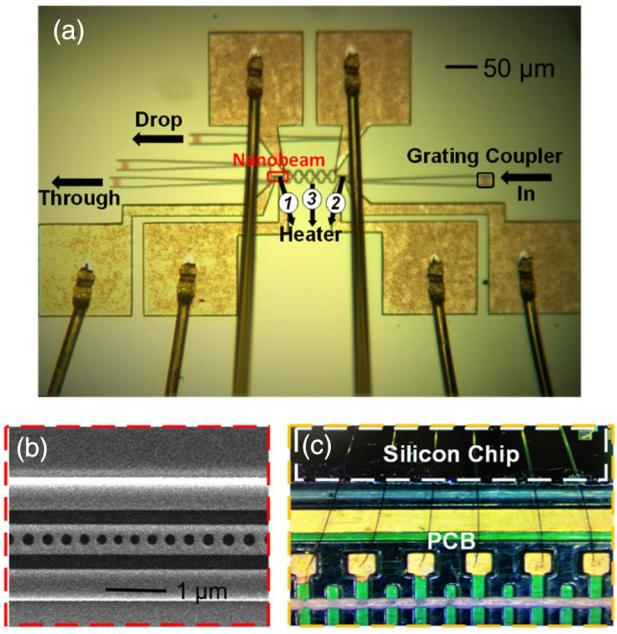

Fig. 3. (a) Micrograph of the fabricated 2 × 2 TO switch based on dual PCN 3W structures. (b) SEM image of the fabricated PCN 3W structure. (c) Device after wire bonding to a PCB.

Figure 3(b) shows the scanning electron microscope (SEM) image of the fabricated PCN 3W structure. In the measurements, the TE-polarized light from a tunable laser scanning from 1570 to 1590 nm was vertically coupled into/out of the chip by grating couplers. The device was wire-bonded to a printed circuit board (PCB) for electrical connections, as shown in Fig. 3(c).

3. EXPERIMENTAL RESULTS AND DISCUSSION

The optical performance of a single PCN 3W structure in our fabricated device is first evaluated, and the corresponding ports are ordered, as shown in Fig. 2(a). As Fig. 4, shows, the extinction ratio of the transmission spectrum at the through port is ~5 dB (red solid line), while the transmission spectra at the drop port (green solid line) and the add port (blue dashed line)

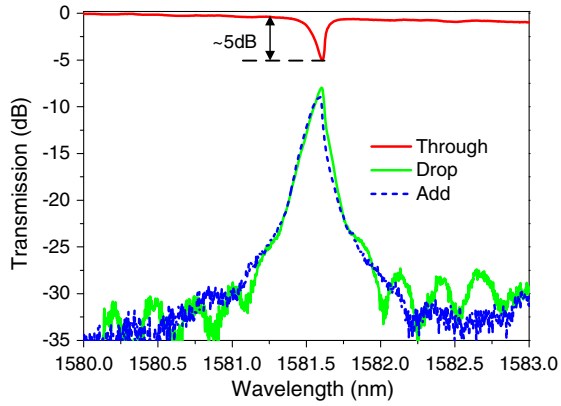

Fig. 4. Transmission spectra of a fabricated single PCN 3W structure in through (red solid), drop (green solid), and add (blue dash) ports. Note that the transmissions are normalized to a reference waveguide and the same to the below measured transmission spectra.

are similar. The experiment results agree with the simulation results in Fig. 2(b): The extinction ratio of ~5 dB is a little less than the theoretical value of ~6 dB due to the fabrication errors.

The transmission spectra of our 2 × 2 TO switch are shown in Fig. 5(a). The solid lines present the initial transmission spectra at different ports. Since the resonance wavelengths of the two PCNs were different due to fabrication errors, a thermal tuning with an applied power of 1.8 mW was used to align the resonance wavelengths. When the resonance wavelengths were aligned at 1583.6 nm (red line with plus symbol), the extinction ratio at the through port increased to ~9 dB. The output power at the drop port (blue line with triangle symbol) also increased and the output power at the add port (green line with circle symbol) decreased. To obtain a high output at the drop port, a π phase difference $|\Phi_1 - \Phi_2|$ between the two arms is needed, and this can be achieved by carefully designing the MZI arms with an ~220 nm length difference to eliminate the need for a heater to tune the relative phase shift. In our experiment, a heater was used simply to provide a full tuning range to characterize the device and compare with the theory. A static heating power of 17.4 mW was applied to heater #3, which can be reduced to zero in theory. Figure 5(b) shows the transmission spectra of the 2 × 2 TO switch when the π phase difference is achieved. The extinction ratio at the through port reaches

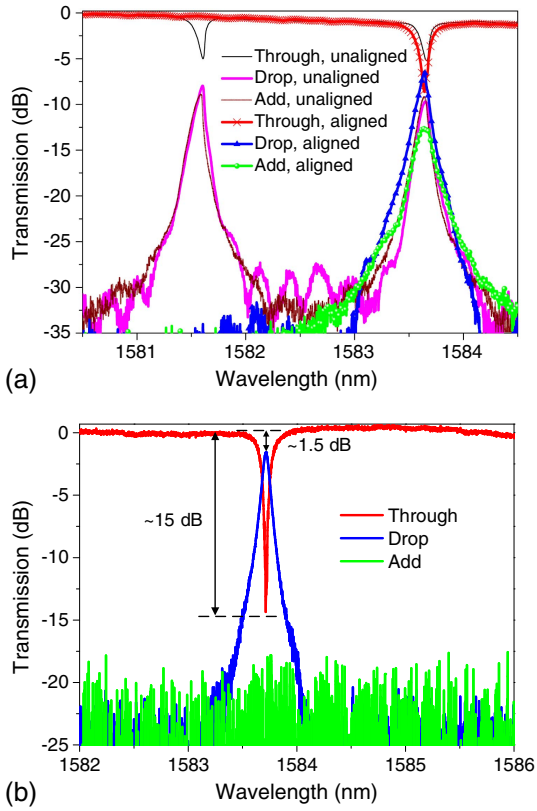

Fig. 5. (a) Transmission spectra of the fabricated 2 × 2 TO switch based on dual PCN 3W structures with the unaligned wavelength state (solid lines) and the aligned wavelength state (lines with symbols). (b) Transmission spectra of the fabricated 2 × 2 TO switch based on dual PCN 3W structures with a π phase difference at through (red line)/drop (blue line)/add (green line) ports.

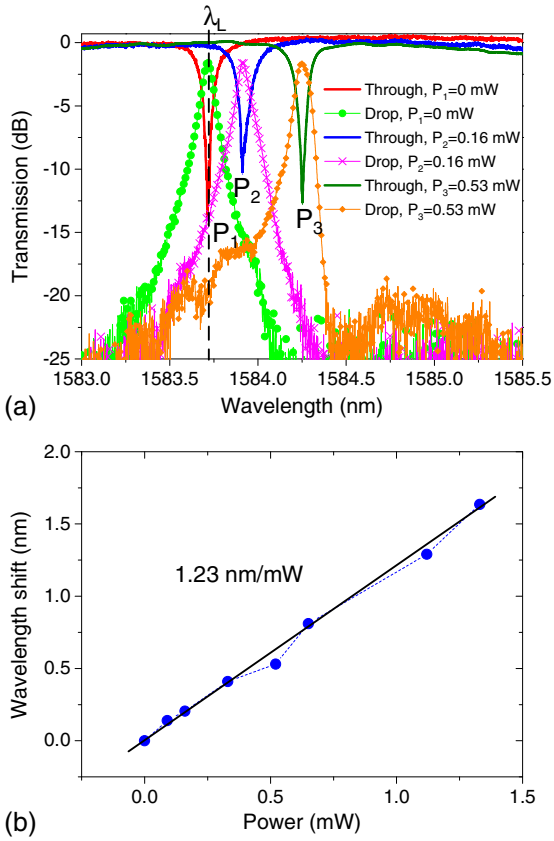

Fig. 6. (a) Transmission spectra of the fabricated 2 × 2 TO switch based on dual PCN 3W structures with various applied powers (P_1, P_2, P_3) at the through ports (solid lines) and the drop ports (lines with symbols). (b) Fitting curve of the resonance wavelength shift of 2 × 2 TO switch based on dual PCN 3W structures as a function of the applied power.

~15 dB and the IL at the drop port is ~1.5 dB at the resonant wavelength of 1583.75 nm. The FWHM of the transmission spectrum at the through port is ~0.09 nm with a quality factor of ~18000.

The TO crossbar switching process was then demonstrated by applying thermal power onto each of the two microheaters on the top of the PCN cavities. The spectra corresponding to three different total powers of 0, 0.16, and 0.53 mW are illustrated in Fig. 6(a). Taking $\lambda_L = 1583.75$ nm as the operation wavelength, ~70% (–1.5 dB) of the input optical power was transmitted to the drop port and the device worked at the cross state if the applied power was $P_1 = 0$ mW. The switch changed to the bar state and ~95% (–0.2 dB) of the optical power went to the through port if the applied power was $P_2 = 0.16$ mW. Thus, only ~0.16 mW is required to change the state from the cross state to the bar state. Here the total power is defined as the increased power on the two PCN cavities after the resonance wavelengths of the PCN cavities are aligned and the π phase difference is obtained. The solid lines and the lines with symbols indicate the transmission spectra of the through port and the drop port, respectively. At the operation wavelength of 1583.75 nm, we then determine the performance metrics of the 2 × 2 switch by inspection of Fig. 6(a), where we find the following results: IL(bar) = –0.2 dB, CT(bar) = –15 dB, IL(cross) = –1.5 dB and CT(cross) = –15 dB. The IL of the switch in the bar state is ~0.2 dB. To characterize the thermal tuning efficiency of the TO switch, the resonance wavelength shift was measured as a function of the power applied on the microheaters, as shown in Fig. 6(b), and the observed TO tuning efficiency is as high as 1.23 nm/mW. Furthermore, response times with a rising time constant of $\tau_{rise} = 3.1$ μs and a falling time constant of $\tau_{fall} = 4.5$ μs were measured in the experiment.

Table 1 provides comparisons of the operational performance of our work versus several recently reported typical on-chip TO switches. The switching power is much lower than that of the TO switches with the silicon-on-silica structures and metal heaters. The proposed device enables a small footprint and high tuning efficiency for the on-chip integrated circuits.

4. CONCLUSION

In conclusion, we have experimentally demonstrated a compact 2 × 2 TO crossbar switch based on dual silicon PCN cavities embedded in 3W directional couplers. The TE-mode optical device was fabricated on an SOI platform with a small device footprint of 30 μm × 150 μm. By thermally tuning the refractive index of the 2 μm silicon central region, the resonance wavelength of the PCN cavities can be red-shifted. Only ~0.16 mW is needed to implement the optical cross-to-bar switching process. We measured IL(bar) = –0.2 dB, CT(bar) = –15 dB, IL(cross) = –1.5 dB, and CT(cross) = –15 dB at 1583.75 nm. The thermal tuning efficiency of our fabricated TO switch is as high as 1.23 nm/mW. With the advantages of a compact device footprint and submilliwatt switching power, the proposed device may have potential applications for next generation compact, low power and reconfigurable wavelength-division multiplexed (WDM) networks.

Table 1. Comparisons of the Operation Performances of Various Silicon TO Switches

Types	Device Footprint	Thermal Tuning Efficiency	Switching Power
Adiabatic bend-based MZI [28]	~5000 μm^2	–	12.7 mW
MRR [29]	~400 μm^2	0.25 nm/mW	3.3 mW
MZI [30]	>10000 μm^2	–	30 mW
Dual MRRs [31]	~1000 μm^2	0.9 nm/mW	6.8 mW
Photonic crystal [32]	35 μm × 10 μm	0.63 nm/mW	18.2 mW
2D waveguide-based MZI [33]	42 μm × 42 μm	–	26 mW
Our work	30 μm × 150 μm	1.23 nm/mW	0.16 mW

Funding. National Natural Science Foundation of China (NSFC) (61235007, 61505104, 61605112); Science and Technology Commission of Shanghai Municipality (15ZR1422800, 16XD1401400); National Key R&D Program of China (2016YFB0402501).

Acknowledgment. We acknowledge the helpful discussions with Richard Soref, and the support of device fabrication by the Center for Advanced Electronic Materials and Devices of Shanghai Jiao Tong University.

REFERENCES

1. X. Wan, N. Hua, and X. P. Zheng, "Dynamic routing and spectrum assignment in spectrum-flexible transparent optical networks," J. Opt. Commun. Netw. **4**, 603–613 (2012).
2. S. J. B. Yoo, "Optical packet and burst switching technologies for the future photonic internet," J. Lightwave Technol. **24**, 4468–4492 (2006).
3. Y. W. Yin, R. Proietti, X. H. Ye, C. J. Nitta, V. Akella, and S. J. B. Yoo, "LIONS: an AWGR-based low-latency optical switch for high-performance computing and data centers," IEEE J. Sel. Top. Quantum Electron. **19**, 3600409 (2013).
4. K. Chen, A. Singla, A. Singh, K. Ramachandran, L. Xu, Y. P. Zhang, X. T. Wen, and Y. Chen, "An optical switching architecture for data center networks with unprecedented flexibility," IEEE/ACM Trans. Netw. **22**, 498–511 (2014).
5. Y. Shoji, K. Kintaka, S. Suda, H. Kawashima, T. Hasama, and H. Ishikawa, "Low-crosstalk 2 × 2 thermo-optic switch with silicon wire waveguides," Opt. Express **18**, 9071–9075 (2010).
6. L. Chen and Y. K. Chen, "Compact, low-loss and low-power 8 × 8 broadband silicon optical switch," Opt. Express **20**, 18977–18985 (2012).
7. S. Nakamura, S. Takahashi, M. Sakauchi, T. Hino, M. Yu, and G. Lo, "Wavelength selective switching with one-chip silicon photonic circuit including 8 × 8 matrix switch," in *Optical Fiber Communication Conference*, OSA Technical Digest (Optical Society of America, 2011), paper OTuM2.
8. S. Zhao, L. Lu, L. Zhou, D. Li, Z. Guo, and J. Chen, "16 × 16 silicon Mach–Zehnder interferometer switch actuated with waveguide micro-heaters," Photon. Res. **4**, 202–206 (2016).
9. R. Yu, S. Cheung, and Y. Li, "A scalable silicon photonic chip-scale optical switch for high performance computing systems," Opt. Express **21**, 32655–32663 (2013).
10. K. Suzuki, K. Tanizawa, T. Matsukawa, G. Cong, S.-H. Kim, S. Suda, M. Ohno, T. Chiba, H. Tadokoro, M. Yanagihara, Y. Igarashi, M. Masahara, S. Namiki, and H. Kawashima, "Ultra-compact 8 × 8 strictly-nonblocking Si-wire PILOSS switch," Opt. Express **22**, 3887–3894 (2014).
11. T. Goh, M. Yasu, and K. Hattori, "Low-loss and high-extinction-ratio silica-based strictly nonblocking 16 × 16 thermooptic matrix switch," IEEE Photon. Technol. Lett. **10**, 810–812 (1998).
12. Q. Xu, B. Schmidt, J. Shakya, and M. Lipson, "Cascaded silicon micro-ring modulators for WDM optical interconnection," Opt. Express **14**, 9430–9435 (2006).
13. R. L. Espinola, M.-C. Tsai, J. T. Yardley, and R. M. Osgood, Jr., "Fast and low-power thermooptic switch on thin silicon-on-insulator," IEEE Photon. Technol. Lett. **15**, 1366–1368 (2003).
14. M. Harjanne, M. Kapulainen, T. Aalto, and P. Heimala, "Sub-μs switching time in silicon-on-insulator Mach–Zehnder thermooptic switch," IEEE Photon. Technol. Lett. **16**, 2039–2041 (2004).
15. I. Kiyat, A. Aydinli, and N. Dagli, "Low-power thermooptical tuning of SOI resonator switch," IEEE Photon. Technol. **18**, 364–366 (2006).
16. X. Wang, J. A. Martinez, M. S. Nawrocka, and R. R. Panepucci, "Compact thermally tunable silicon wavelength switch: modeling and characterization," IEEE Photon. Technol. Lett. **20**, 936–938 (2008).
17. Z. Zhou, B. Yin, Q. Deng, X. Li, and J. Cui, "Lowering the energy consumption in silicon photonic devices and systems," Photon. Res. **3**, B28–B45 (2015).
18. W. Fegadolli, J. Oliveira, V. Almeida, and A. Scherer, "Compact and low power consumption tunable photonic crystal nanobeam cavity," Opt. Express **21**, 3861–3871 (2013).
19. Q. Quan, D. Floyd, I. Burgess, P. Deotare, I. Frank, S. Tang, R. Ilic, and M. Loncar, "Single particle detection in CMOS compatible photonic crystal nanobeam cavities," Opt. Express **21**, 32225–32233 (2013).
20. Q. Quan and M. Loncar, "Deterministic design of wavelength scale, ultra-high *Q* photonic crystal nanobeam cavities," Opt. Express **19**, 18529–18542 (2011).
21. C. V. Poulton, X. Zeng, M. T. Wade, J. M. Shainline, J. S. Orcutt, and M. A. Popović, "Photonic crystal microcavities in a microelectronics 45 nm SOI CMOS Technology," IEEE Photon. Technol. Lett. **27**, 665–668 (2015).
22. K. Nozaki, T. Tanabe, A. Shinya, S. Matsuo, T. Sato, H. Taniyama, and M. Notomi, "Sub-femtojoule all-optical switching using a photonic-crystal nanocavity," Nat. Photonics **4**, 477–483 (2010).
23. X. Ge, Y. Shi, and S. He, "Ultra-compact channel drop filter based on photonic crystal nanobeam cavities utilizing a resonant tunneling effect," Opt. Lett. **39**, 6973–6976 (2014).
24. H. Zhou, C. Qiu, J. Wu, B. Liu, X. Jiang, J. Peng, Z. Xu, R. Liu, Y. Zhang, Y. Su, and R. Soref, "2 × 2 electro-optic switch with fJ/bit switching power based on dual photonic crystal nanobeam cavities," in *Proceedings of Conference on Lasers and Electro-Optics (CLEO)* (2016), paper JTh2A.24.
25. H. Zhou, C. Qiu, Z. Xu, X. Jiang, Y. Yang, L. Han, Y. Zhang, and Y. Su, "A 2 × 2 silicon thermo-optic switch based on nanobeam cavities with ultra-small mode volumes," in *Proceedings of International Conference on Group IV Photonics* (2016) paper WB5.
26. C. Manolatou, M. J. Khan, S. Fan, P. Villeneuve, H. Haus, and J. Joannopoulos, "Coupling of modes analysis of resonant channel add-drop filters," IEEE J. Quantum Electron. **35**, 1322–1331 (1999).
27. C. V. Poulton, X. Zeng, M. T. Wade, and M. A. Popović, "Channel add-drop filter based on dual photonic crystal cavities in push-pull mode," Opt. Lett. **40**, 4206–4209 (2015).
28. M. R. Watts, J. Sun, C. DeRose, D. C. Trotter, R. W. Young, and G. N. Nielson, "Adiabatic thermo-optic Mach–Zehnder switch," Opt. Lett. **38**, 733–735 (2013).
29. Q. Li, D. Nikolova, D. M. Calhoun, Y. Liu, R. Ding, and T. B. Jones, "Single microring-based 2 × 2 silicon photonic crossbar switches," IEEE Photon. Technol. Lett. **27**, 1981–1984 (2015).
30. K. Suzuki, G. Cong, K. Tanizawa, S. Kim, K. Ikeda, S. Namiki, and H. Kawashima, "Ultra-high-extinction-ratio 2 × 2 silicon optical switch with variable splitter," Opt. Express **23**, 9083–9092 (2015).
31. P. Dong, W. Qian, H. Liang, R. Shafiiha, N. Feng, D. Feng, X. Zheng, A. V. Krishnamoorthy, and M. Asghari, "Low power and compact reconfigurable multiplexing devices based on silicon microring resonators," Opt. Express **18**, 9852–9858 (2010).
32. X. Zhang, S. Chakravarty, C. Chung, Z. Pan, H. Yan, and R. T. Chen, "Ultra-compact and wide-spectrum-range thermo-optic switch based on silicon coupled photonic crystal microcavities," Appl. Phys. Lett. **107**, 221104 (2015).
33. K. Liu, C. Zhang, S. Mu, S. Wang, and V. J. Sorger, "Two-dimensional design and analysis of trench-coupler based Silicon Mach–Zehnder thermo-optic switch," Opt. Express **24**, 15845–15853 (2016).